symmetry

Article

β-Delayed γ Emissions of ^{26}P and Its Mirror Asymmetry

Hao Jian [1,2,†], Yufeng Gao [1,3,†], Fanchao Dai [1,2], Jiajian Liu [1], Xinxing Xu [1,2,4,5,6,*], Cenxi Yuan [3,*], Kazunari Kaneko [7], Yang Sun [1,5,8], Pengfei Liang [4], Guozhu Shi [1,2,9], Lijie Sun [5,8], Latsamy Xayavong [10], Chengjian Lin [5,11], Jenny Lee [4], Zhihuan Li [12], Yanyun Yang [1,2], Pengjie Li [1,4], Rui Fan [1,2], Sixian Zha [1,2], Haofan Zhu [1,2], Jinhai Li [1,2], Qirui Gao [1], Zhaozhan Zhang [1,3], Ruofu Chen [1], Jiansong Wang [1,13], Dongxi Wang [5], Hongyi Wu [12], Kang Wang [1,14], Yihua Lam [1,2], Fangfang Duan [1,2,9], Peng Ma [1], Zhihao Gao [1,9], Qiang Hu [1], Zhen Bai [1], Junbing Ma [1], Jianguo Wang [1], Fupeng Zhong [5,11], Chenguang Wu [12], Diwen Luo [12], Ying Jiang [12], Yang Liu [12], Dongsheng Hou [1,2], Ren Li [1,2], Nanru Ma [5], Weihu Ma [1,15], Gongming Yu [1,16], Dipika Patel [1,17], Shuya Jin [1,2], Yufeng Wang [1,18], Yuechao Yu [1,18], Qingwu Zhou [1,19], Peng Wang [1,19], Liyuan Hu [16], Xiang Wang [12], Hongliang Zang [12], Qingqing Zhao [4], Lei Yang [5], Peiwei Wen [5], Feng Yang [5], Huiming Jia [5], Gaolong Zhang [20], Min Pan [5,20], Xiaoyu Wang [20], Haohan Sun [5], Meng Wang [1,2,6], Zhengguo Hu [1,2,6], Xiaohong Zhou [1,2,6], Yuhu Zhang [1,2,6], Hushan Xu [1,2,6], Minliang Liu [1], Hooi-Jin Ong [1,2,21,22] and Weiqing Yang [1]

1 CAS Key Laboratory of High Precision Nuclear Spectroscopy, Institute of Modern Physics, Chinese Academy of Sciences, Lanzhou 730000, China; jianhao19@mails.ucas.ac.cn (H.J.); gaoyf0923@163.com (Y.G.); daifanchao20@mails.ucas.ac.cn (F.D.); liujj@impcas.ac.cn (J.L.); sunyang@sjtu.edu.cn (Y.S.); sgz12sgz@impcas.ac.cn (G.S.); yangyanyun@impcas.ac.cn (Y.Y.); lipengjie@impcas.ac.cn (P.L.); fanrui20@mails.ucas.ac.cn (R.F.); zhasixian20@mails.ucas.ac.cn (S.Z.); zhuhaofan21@mails.ucas.ac.cn (H.Z.); lijinhai21@mails.ucas.ac.cn (J.L.); gaoqr@impcas.ac.cn (Q.G.); zhangchzh@mail2.sysu.edu.cn (Z.Z.); chenruofu@impcas.ac.cn (R.C.); wjs@zjhu.edu.cn (J.W.); wangkang@impcas.ac.cn (K.W.); lamyihua@gmail.com (Y.L.); duanfangfang@impcas.ac.cn (F.D.); mapeng@impcas.ac.cn (P.M.); zhihao.gao@physics.uu.se (Z.G.); qianghu@impcas.ac.cn (Q.H.); baizh@impcas.ac.cn (Z.B.); jnbm@impcas.ac.cn (J.M.); wangjg@impcas.ac.cn (J.W.); ytdxahou@163.com (D.H.); ren.li@csnsm.in2p3.fr (R.L.); maweihu@fudan.edu.cn (W.M.); ygmanan@uw.edu (G.Y.); kherdipika2006@gmail.com (D.P.); jinshuya@impcas.ac.cn (S.J.); yf_wang21@163.com (Y.W.); henanyyz@163.com (Y.Y.); qwzhou2021@163.com (Q.Z.); wang_peng21@163.com (P.W.); wangm@impcas.ac.cn (M.W.); huzg@impcas.ac.cn (Z.H.); zxh@impcas.ac.cn (X.Z.); yhzhang@impcas.ac.cn (Y.Z.); hushan@impcas.ac.cn (H.X.); liuml@impcas.ac.cn (M.L.); onghjin@impcas.ac.cn (H.-J.O.); ywq@impcas.ac.cn (W.Y.)
2 School of Nuclear Science and Technology, University of Chinese Academy of Sciences, Beijing 100049, China
3 Sino-French Institute of Nuclear Engineering and Technology, Sun Yat-Sen University, Zhuhai 519082, China
4 Department of Physics, The University of Hong Kong, Hong Kong, China; liangpf@connect.hku.hk (P.L.); jleehc@hku.hk (J.L.); cyanzhao@connect.hku.hk (Q.Z.)
5 Department of Nuclear Physics, China Institute of Atomic Energy, Beijing 102413, China; sunli@frib.msu.edu (L.S.); cjlin@ciae.ac.cn (C.L.); wangdongxi@ciae.ac.cn (D.W.); zhongfupeng@ciae.ac.cn (F.Z.); mnr209@163.com (N.M.); yang_lei@ciae.ac.cn (L.Y.); wenpeiwei@hotmail.com (P.W.); martin@ciae.ac.cn (F.Y.); jiahm@ciae.ac.cn (H.J.); panminaiwuli@163.com (M.P.); haohansun@126.com (H.S.)
6 Advanced Energy Science and Technology Guangdong Laboratory, Huizhou 516003, China
7 Department of Physics, Kyushu Sangyo University, Fukuoka 813-8503, Japan; kaneko@ip.kyusan-u.ac.jp
8 School of Physics and Astronomy, Shanghai Jiao Tong University, Shanghai 200240, China
9 School of Nuclear Science and Technology, Lanzhou University, Lanzhou 730000, China
10 Department of Physics, Faculty of Natural Sciences, National University of Laos, Vientiane 01080, Laos; xayavong.latsamy@gmail.com
11 College of Physics and Technology, Guangxi Normal University, Guilin 541004, China
12 State Key Laboratory of Nuclear Physics and Technology, School of Physics, Peking University, Beijing 100871, China; zhli@pku.edu.cn (Z.L.); wuhongyi@pku.edu.cn (H.W.); yuanfangsee@pku.edu.cn (C.W.); luodiwen@pku.edu.cn (D.L.); jytot@pku.edu.cn (Y.J.); liuyang_enphy@pku.edu.cn (Y.L.); wxsyhwl@pku.edu.cn (X.W.); zhl13@pku.edu.cn (H.Z.)
13 College of Science, Huzhou University, Huzhou 313000, China
14 Shanghai Institute of Applied Physics, Chinese Academy of Sciences, Shanghai 201800, China
15 Institute of Modern Physics, Fudan University, Shanghai 200433, China
16 Fundamental Science on Nuclear Safety and Simulation Technology Laboratory, Harbin Engineering University, Harbin 150001, China; huliyuan@hrbeu.edu.cn
17 Department of Physics, Sardar Vallabhbhai National Institute of Technology, Surat 395007, India
18 School of Physics and Astronomy, Yunnan University, Kunming 650091, China
19 School of Physical Science and Technology, Southwest University, Chongqing 400044, China

check for updates

Citation: Jian, H.; Gao, Y.; Dai, F.; Liu, J.; Xu, X.; Yuan, C.; Kaneko, K.; Sun, Y.; Liang, P.; Shi, G.; et al. β-Delayed γ Emissions of ^{26}P and Its Mirror Asymmetry. *Symmetry* **2021**, *13*, 2278. https://doi.org/10.3390/sym13122278

Academic Editors: Yu-Gang Ma, De-Qing Fang and Fu-Rong Xu

Received: 26 October 2021
Accepted: 20 November 2021
Published: 30 November 2021

[20] School of Physics and Nuclear Energy Engineering, Beihang University, Beijing 100191, China; zgl@buaa.edu.cn (G.Z.); sy1619140@buaa.edu.cn (X.W.)
[21] Research Center for Nuclear Physics, Osaka University, Osaka 567-0047, Japan
[22] Joint Department for Nuclear Physics, Lanzhou University and Institute of Modern Physics, CAS, Lanzhou 730000, China
* Correspondence: xinxing@impcas.ac.cn (X.X.); yuancx@mail.sysu.edu.cn (C.Y.)
† These authors contributed equally to this work and should be considered as co-first authors.

Abstract: The study of the origin of asymmetries in mirror β decay is extremely important to understand the fundamental nuclear force and the nuclear structure. The experiment was performed at the National Laboratory of Heavy Ion Research Facility in Lanzhou (HIRFL) to measure the β-delayed γ rays of ^{26}P by silicon array and Clover-type high-purity Germanium (HPGe) detectors. Combining with results from the β decay of ^{26}P and its mirror nucleus ^{26}Na, the mirror asymmetry parameter δ ($\equiv ft^{+}/ft^{-} - 1$) was determined to be 46(13)% for the transition feeding the first excited state in the daughter nucleus. Our independent results support the conclusion that the large mirror asymmetry is close to the proton halo structure in ^{26}P.

Keywords: isospin symmetry breaking; β-delayed γ decay; shell-model calculation; halo structure; clover-type HPGe detector

1. Introduction

In 1932, Heisenberg introduced the elegant concept of isospin, which described the charge-independence of nucleons in nuclei, namely, he considered protons and neutrons the same particles in different states [1]. This has been proven valuable in simplifying the construction of the nucleon–nucleon interactions in nuclear models, as well as in describing both systematic and specific features of nuclear structures [2]. However, because of the differences in mass and electromagnetic interaction between a proton and a neutron, the concept of isospin symmetry is approximate. Isospin symmetry breaking caused by the Coulomb force acting between protons and other isospin nonconserving (INC) forces [3] frequently implies new physics, and the systematic study of the origin of breaking is extremely important for a deeper understanding of the fundamental nuclear force and the nuclear structure. In a recent study, the evidence of mirror-symmetry violation for the ground state within the ^{73}Br/^{73}Sr partners was reported [4]. The ground states of the particle-bound nuclei ^{73}Sr and ^{73}Br appeared to have J^{π}=5/2^{-} and J^{π}=1/2^{-}, respectively. The breaking of symmetry was probably revealed by an inversion of states, this observation offering insights into charge-symmetry breaking forces acting in atomic nuclei.

Investigating β decays of mirror nuclei which have the interchanged number of protons and neutrons is of fundamental importance in nuclear and particle physics, since it directly addresses the isospin symmetry problems. In Gamow–Teller (GT) transitions, the reduced transition probability ($ft^{\pm}$) values can be extracted to define the mirror asymmetry parameter:

$$\delta = \frac{ft^{+}}{ft^{-}} - 1, \tag{1}$$

where the ft^{+} and ft^{-} values are associated with the β^{+} decay and the β^{-} decay of the mirror pair, respectively. The δ also describes the extent of isospin-symmetry breaking [5]. Large asymmetries in mirror Gamow–Teller transitions have been associated with transitions involving halo states [6]. So as to systematically study the isospin symmetry breaking, β decays of the *sd* shell mirror nuclei near the proton drip line have been investigated [7–15]. The largest value of mirror asymmetry (δ = 209(96)%) in low-lying states in ^{22}Si/^{22}O was found in a recent paper [8], supporting the proton halo in ^{22}Al. For the extremely proton-rich phosphorus isotopes, the mirror asymmetry parameters in ^{26}P/^{26}Na partners was observed to be 51(10)% [14].

The INC forces related to the $s_{1/2}$ orbit, commonly adopted to interpret isospin-symmetry breaking for the nuclei in *sd* shell, were used to reproduce the large mirror asymmetry between ^{26}P and ^{26}Na [5]. These results support the conclusion that ^{26}P is a candidate nucleus with a proton halo. In addition, the low separation energy of ^{26}P with narrow momentum distribution and enhanced cross section observed in proton-knockout reactions was associated with the existence of a proton halo in ^{26}P. In this paper, we present the independent and rather complete results of the β-delayed γ decay of ^{26}P. The mirror asymmetries were discussed concerning the shell-model calculation.

2. Experimental Setup

The experiment was performed at the Heavy Ion Research Facility of Lanzhou (HIRFL) [16] in November 2017. The secondary radioactive ions were produced via the projectile fragmentation of the $^{32}S^{16+}$ beam impinging on a 1581-µm-thick ^{9}Be target, which was accelerated to 80.6 MeV/nucleon at intensity of ∼87 *e*nA (∼5.4 *p*nA) using the K69 Sector Focus Cyclotron and the K450 Separate Sector Cyclotron. The Radioactive Ion Beam Line in Lanzhou (RIBLL1) [17] was a powerful tool concerning optimization and selection of ^{26}P.

The particle identification was done by the combination of energy loss (ΔE), time of flight (ToF), and magnetic rigidity ($B\rho$), shown in Figure 1, according to the LISE++ simulation [18]. The ToF was measured by two plastic scintillators (T1,T2), and the ΔE was measured by two silicon detectors ($\Delta E1$, $\Delta E2$). The correlations using energy and time signals were applied to acquire the valid number of implanted ^{26}P ions from contaminants.

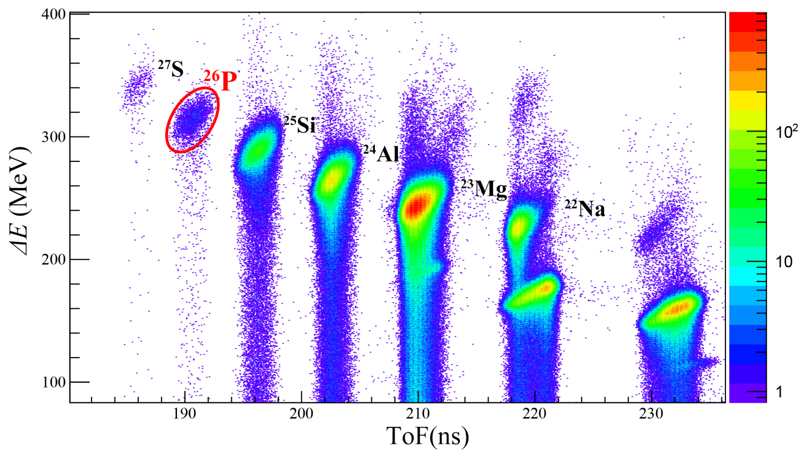

Figure 1. Two-dimensional identification plot of ΔE and ToF for the ions in the secondary beam. The heavy ions of ^{26}P are marked with a red circle. The others are marked with the corresponding isotope symbols.

The detection system reported in reference [19] consisted of three double-sided silicon strip detectors (DSSDs) [20] backed by three quadrant silicon detectors (QSDs) [21] surrounded by five clover-type high-purity germanium (HPGe) detectors and three lanthanum bromide detectors. The different thicknesses of the detectors are given in Table 1. A series of measurement techniques, such as circulating alcohol cooling, constant fraction timing, and front and back coincidence of DSSDs, were used to improve the signal-to-noise ratio and the accurate measurement of decay events with high detection efficiency and low detection energy threshold [22].

Table 1. The thickness of different detectors used in this experiment.

Detectors	DSSD1	DSSD2	DSSD3	QSD1	QSD2	QSD3
Thickness (µm)	142	40	304	1546	300	300
Area(mm^2)	49.5 × 49.5	49.5 × 49.5	49.5 × 49.5	50 × 50	50 × 50	50 × 50

The 304-μm-thick DSSD3 was an important supplement to DSSD2 due to a higher detection efficiency for high-energy protons and β particles. QSDs of different thicknesses were set in the downstream of the beam, in which 1546-μm-thick QSD1 was used to detect β particles and take protons escaping from DSSDs into account. Besides, 300-μm-thick QSD2 and QSD3 were located at the very end of the beam and used to serve as anti-coincident detectors for light particles. The surrounding Clover-type HPGe detectors were placed outside the silicon detectors to measure γ rays emitted after the β decay.

The SPA02- and SPA03-type charge sensitive amplifiers (CSAs) [22] were assembled in all the silicon detectors. Since the three DSSDs are needed to measure high-energy implanting signals and low-energy decaying signals simultaneously, the output signals of the preamplifiers via 16 printed circuit board (PCBs) feedthroughs were split into two different amplitudes. The data acquisition system PKU DAQ was triggered by the implantation or decay signals of the three DSSDs. The DAQ system was adapted from the RIBF DAQ [23]. More detailed information concerning this experiment is given in reference [9].

Our experimental setup was quite similar to the one by J.C.Thomas [24]. Because of more implanting DSSDs and surrounding HPGe detectors, we got more accurate data as well as the position information and the β-delayed particles simultaneously. Not only that, we also measured and calculated the $^{25}Al(p,\gamma)^{26}Si$ reaction rate [19]. Focusing mainly on the β-delayed γ rays, germanium double-sided strip detectors (GeDSSDs) and 16 SeGA detectors were used in the experiment by Pérez-Loureiro [14]. So the partial branching ratio of the γ ray was slightly more accurate than ours.

3. Data Analysis and Experimental Results

In continuous beam mode, the nuclei of interest were stopped by DSSDs. The total thickness of Al degraders in this experiment was set as 220 μm so that the proportions of ^{26}P ions stopped in DSSD2 and DSSD3 were approximately equal. The high energy calibrations of three DSSDs could be performed by the secondary beam combined with LISE ++ calculations [18], and then the particle energies were converted to the implanted depths using the SRIM program [25]. The secondary beam was scattered through multiple sets of Al degrader, making the distribution of ^{26}P more uniform across the silicon surface. Figure 2 shows the surface distributions of ^{26}P implanted on DSSD3 in the x-y axis. The stopped position of each ^{26}P particle could be determined by the x-y information to obtain the original position of each decay particle. The total number of ^{26}P implantations in DSSD1, DSSD2, DSSD3 were 6954, 139,308, and 139,801, respectively.

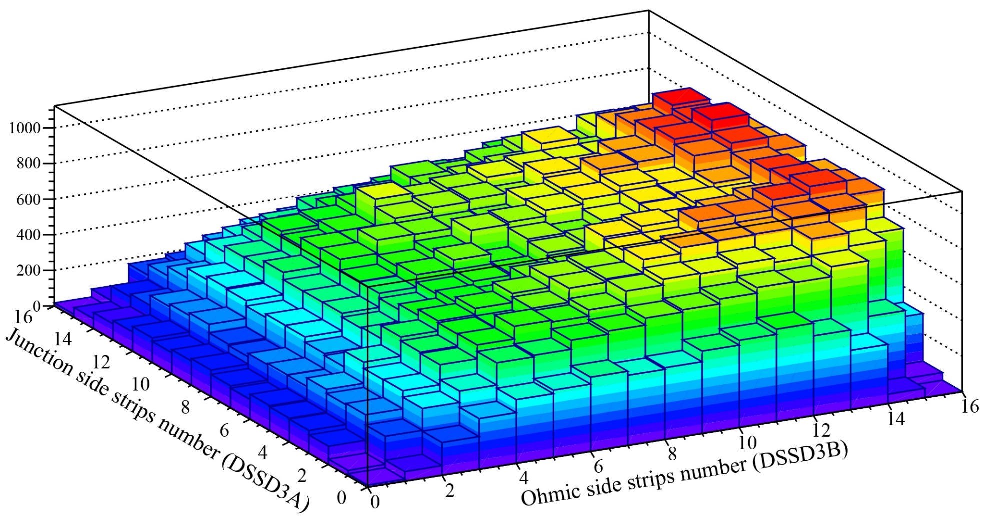

Figure 2. The surface distributions of ^{26}P ions implanted on DSSD3 in the x-y axis.

3.1. Half-Life

Each DSSD was divided into 16 × 16 pixels, and the correlations were based on the time difference between the implantation events and the decay events recorded in the same pixel. The decay-time spectrum is shown in Figure 3. Most of the implantation events were correlated with the decay events under the high implanting rate beam condition, except for a relatively small number of noise or background events which would form a constant background on the decay-time spectrum. The fitting was performed by Maximum Likelihood Fitting (MLF) [26]. The fitting expression is shown in the following:

$$N(t) = Ae^{\frac{-tln2}{T_{1/2}}} + B \tag{2}$$

where $N(t)$ is the total number of ions decaying in unit time, t is the decay time, A is the number of ions decaying at the beginning, B is the constant background in the decay, and $T_{1/2}$ is the half-life. The half-life of ^{26}P was deduced to be $T_{1/2}$ = 43.7 ± 0.3 ms with the error of the fitting uncertainty (including statistical error), which is in good agreement with the literature value of 43.7 ± 0.6 ms given by J.C.Thomas et al. [24].

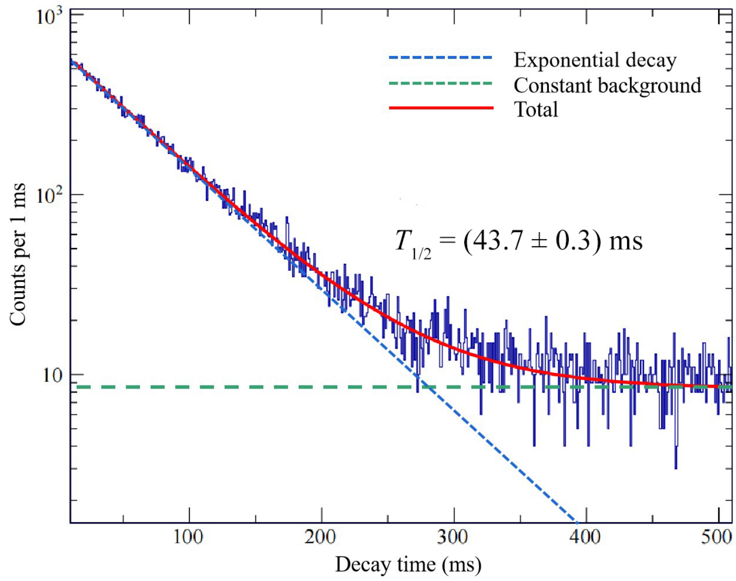

Figure 3. The decay-time spectrum of ^{26}P.

3.2. β-Delayed γ Rays

In this experiment, five Clover-type HPGe detectors were installed to measure γ rays. The β-γ detection efficiency was defined by the product of the detection efficiency of β particles in DSSDs and the detection efficiency of γ rays in the Clover-type HPGe detectors. Since the thickness of DSSD3 (304 μm) is much larger than that of DSSD1 (142 μm) and DSSD2 (40 μm), only the β signal in DSSD3 and the corresponding γ rays recorded by the Clover-type HPGe detectors were used for the calibration of the β-γ detection efficiency. The number of β-delayed γ rays observed at energy E is

$$N_\gamma(E) = N_0 \times \varepsilon_{\beta\gamma}(E) \times I_\gamma(E) \tag{3}$$

where N_0 is the total number of ions stopped in DSSD3, $\varepsilon_{\beta\gamma}$ is the β-γ detection efficiency parametrized by $\varepsilon = aE^b$, and I_γ is the absolute γ-ray intensity. The β-γ detection efficiency was obtained by 452 keV (18.4(42)%), 493 keV (15.3(34)%), 945 keV (10.4(23)%), 1612 keV (15.2(32)%) from ^{25}Si [24] and 1248.5 keV (38.2(69)%),1985.6 keV (31.1(54)%), 2062.3 keV (34.1(58)%) from ^{22}Al [27] β-delayed γ rays.

Figure 4 shows the γ spectrum coincided with β particles in the decay of ^{26}P. Fifteen peaks were identified, of which 13 labeled γ_1–γ_{13} are directly related to the decay of ^{26}P.

The total uncertainty was associated with the fitting uncertainty and the calibration of detectors. Statistically, the significant peak in the spectrum is the well-known 511 keV γ ray originated from the positron–electron annihilation. The 1367 keV ray is assigned as the deexcitation from the first 2^+ excited state to the ground state of ^{24}Mg. The detailed information of the β-delayed γ-ray transitions are listed in Table 2.

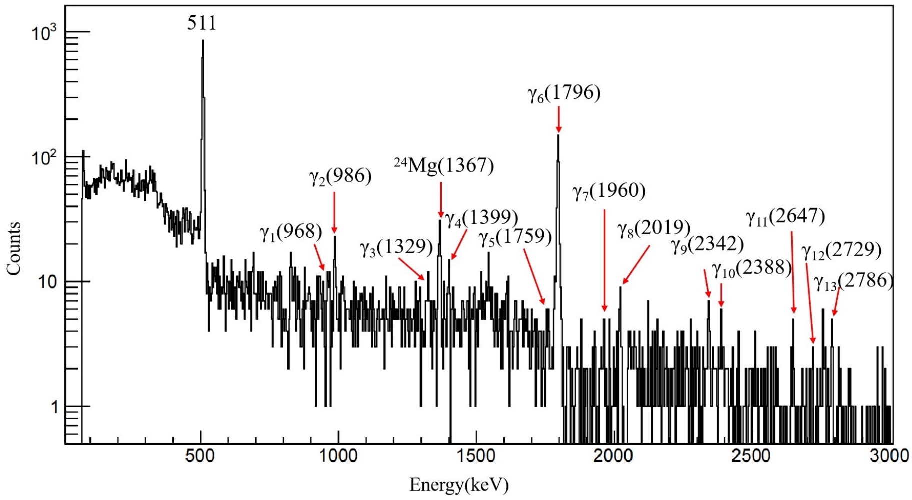

Figure 4. γ-ray spectrum of ^{26}P in coincidence with a β particle from ^{26}P decay. Peaks have been labeled by the energy.

Table 2. Data on the β-delayed γ-rays of ^{26}P. Total 13 γ peaks have been identified.

Peak	E_γ (keV)	I_γ (%)	$J^\pi_{(i)}$	$J^\pi_{(f)}$	E^*_i (keV)	E^*_f (keV)
γ_1	968.6(7)	1.5(3)	3^+	2^+	3756.5(3)	2786(1)
γ_2	986.6(7)	5.7(9)	2^+	2^+	2786(1)	1796.1(2)
γ_3	1329.4(6)	1.4(3)	4^+	3^+	5515.8(6)	4185.4(11)
γ_4	1399.4(6)	3.5(15)	3^+	2^+	4185.4(11)	2786(1)
γ_5	1759.3(6)	0.3(1)	4^+	3^+	5515.8(6)	3756.5(3)
γ_6	1796.1(2)	58(3)	2^+	0^+	1796.1(2)	0
γ_7	1960.4(9)	1.6(5)	3^+	2^+	3756.5(3)	1796.1(2)
γ_8	2019.6(5)	3.2(14)	2^+	2^+	4805.6(11)	2786(1)
γ_9	2342.3(9)	5.1(10)	2^+	2^+	4138.4(9)	1796.1(2)
γ_{10}	2388.4(6)	1.5(4)	3^+	2^+	4185.4(11)	1796.1(2)
γ_{11}	2647.9(4)	1.0(4)	4^+	2^+	4444.0(4)	1796.1(2)
γ_{12}	2729.5(4)	0.6(3)	4^+	2^+	5515.8(6)	2786(1)
γ_{13}	2786(1)	3.7(7)	2^+	0^+	2786(1)	0

3.3. Discussion

Excitation energies of the low-lying proton-bound states in ^{26}Si were deduced by the measured γ ray energies. The branching ratio of the proton-bound excited energy level was deduced from the related γ-ray intensities:

$$BR = I_{out} - I_{in} \tag{4}$$

where I_{out} (I_{in}) is the total intensity of γ ray observed decaying from (feeding to) the energy level in the present experiment.

The β-feeding intensity to the 1796 keV state of ^{26}Si was determined to be BR_1 = 43.1(34)% by extracting the intensities of the 968.6(7)-, 986.6(7)-, 1796.1(2)-, 2342.3(9)-, 2388.4(6)-, and 2647.9(4)-keV γ rays. Because of the large uncertainty, the intensity of the 2782 keV excited state could not be determined. Figure 5 shows the partial decay scheme of ^{26}P deduced from present experiment data comparing with mirror nuclei ^{26}Na in corresponding energy levels.

In order to investigate the isospin asymmetry, we compared the Gamow–Teller decays between the mirror partners. The corresponding $logft$ value for each state of ^{26}Si was calculated using the LOGFT analysis program provided by the NNDC website [28] incorporating the half-life, the excitation energies, the β feeding intensities, and β-decay energy (Q_{EC}/Q_{β^-}). The mirror asymmetries for the first 2^+ excited states between ^{26}Si and ^{26}Mg, extracted from experimental data of the present work and the mirror nucleus ^{26}Na, is 46(13)%, which is in good agreement with the literature value of 51(10)% [14]. For the 3_1^+ and the 2_3^+ states between ^{26}Si and ^{26}Mg, the mirror asymmetry parameter are $-19(19)$% and $-31(15)$%, respectively, as shown in Table 3. Due to the low branching ratio, we did not calculate the mirror asymmetry parameter for the 4^+ excited state. The mirror energy difference (MED) represents the degree of energy differences between the $T_Z = \pm T$ states for the mirror nuclei [29,30]:

$$MED = E_x(I, T, T_Z = -T) - E_x(I, T, T_Z = T) \quad (5)$$

where $E_x(I, T, T_Z = -T)$ is the excitation energy of the states of spin I and isospin T, T_z. The data are listed in Table 3.

Table 3. Comparison between the transitions in the mirror β decays of ^{26}P/^{26}Na.

	^{26}P($\beta\gamma$) ^{26}Si, $T_Z = -2$			**^{26}Na($\beta\gamma$) ^{26}Mg, $T_Z = 2$**				
	$T_{1/2}$ = 43.7(3) ms, Q_{EC} = 18,258(90) keV			**$T_{1/2}$ = 1.07128(25) s, Q_{β^-} = 9354(4) keV** [31]				
J_i^π	**^{26}Si E* (keV)**	**BR (%)**	**log (ft^+)**	**^{26}Mg E* (keV)**	**BR (%)**	**log (ft^-)**	**δ (%)**	**MED**
2_1^+	1796.1(2)	43.1(34)	4.88(4)	1808.81(16)	87.80(7)	4.7148(12)	46(13)	−13(16)
3_1^+	3756.5(3)	2.8(6)	5.78(10)	3941.48(17)	1.31(4)	5.870(14)	−19(19)	−185(17)
2_3^+	4138.4(9)	5.1(10)	5.46(9)	4332.02(17)	1.65(3)	5.62(1)	−31(15)	−180(21)
3_2^+	4185.4(11)	3.6(16)	5.6(2)	4350.02(17)	3.17(7)	5.33(1)	86(86)	−165(20)

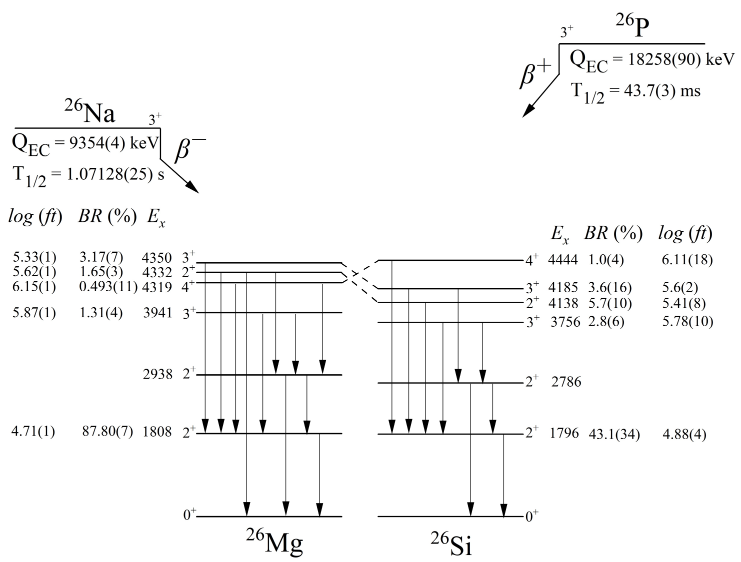

Figure 5. (Left) Partial decay scheme of mirror nuclei ^{26}Na. (Right) Partial decay scheme of ^{26}P deduced from present experiment data.

In a pure Gamow–Teller transition, the ft value is related to the nuclear matrix element through the expression:

$$ft = \frac{K}{(\frac{g_A}{g_V})^2 B_{GT}} \tag{6}$$

where K is a constant, g_V and g_A are the free-vector and axial-vector coupling constants of the weak interaction, and B_{GT} is the Gamow–Teller reduced transition probabilities [32]. Therefore, the mirror asymmetry parameter δ could be expressed in another way through

$$\delta = \frac{ft^+}{ft^-} - 1 = \frac{B^-_{GT}}{B^+_{GT}} - 1 = \frac{\Delta B_{GT}}{B^+_{GT}} \tag{7}$$

where the deviation ΔB_{GT} is defined as $\Delta B_{GT} = B^-_{GT} - B^+_{GT}$.

The properties of *sd* shell nuclei were studied by the Hamiltonian including USD [33,34], USDA, and USDB [35], which are represented in Table 4. Each of these three Hamiltonians are isospin symmetric with zero values of δ. Because of the weakly bound nature of proton $s_{1/2}$ orbit, it is suggested both one- and two-body parts of Hamiltonian should be modified [36]. After modification, MED is well reproduced in mirror partners around A = 20. In the present work, only the transition to the first 2^+ state is concentrated because the absolute values of other B_{GT} transitions are small. The δ values feeding the first 2^+ excited state are 22%, 17%, and 16% given by modified USD, USDA and USDB, respectively (WBE1 in Table 4). The shell-model calculations do not agree with the experimental results perfectly. Actually, the WBE should be considered in not only the Hamiltonian but also the overlap of the wave function. If the proton $s_{1/2}$ orbit in the Gamow–Teller transition is weakly bound while the neutron $s_{1/2}$ orbit is not, the overlap of their wave functions is smaller than one. Considering both weakly bound effects in both the Hamiltonian and the wave function, the δ are corrected to 55%, 51%, and 49% (WBE2 in Table 4), fitting well with the experimental value 46(13)%.

Generally, the large mirror asymmetries were caused by those nuclei where more protons occupy the $s_{1/2}$ orbit near the proton drip line. This also explains that those nuclei have a smaller proton separation energy than the neutron separation energy in their mirror nuclei. The mirror asymmetry known as the Thomas–Ehrman shift [37,38] corresponds to the reduction of the Coulomb energy caused by the spatial expansion of the s-wave proton. The total Hamiltonian, including the Coulomb energies for protons, the single-particle energy shifts resulting from the spin-orbit interaction for both protons and neutrons, and the isospin-nonconserving (INC) forces are usually theoretically discussed to intepret the problems of mirror asymmetry [3]. Thus, the calculation concerning INC forces associated with the $s_{1/2}$ orbit are important to explain the large mirror asymmetry. The quantitative calculation including the $T = 1$, $J = 2, 3$ INC forces by Kaneko and Sun [5] reproduced the results in ^{26}P/^{26}Na.

Table 4. Comparison of calculated δ values using different Hamiltonian for the first 2^+ excited state.

Hamiltonian	δ		
	Origin	**WBE1**	**WBE2**
USD	0%	22%	55%
USDA	0%	17%	51%
USDB	0%	16%	49%

From the above results, it could be concluded that the Coulomb force acting between protons and other INC forces would lead to an extended proton wave function and give rise to mirror asymmetry when approaching the proton drip line.

4. Conclusions

In the present work, the experiment was carried out using the RIBLL1 facility at HIRFL to study the β decays of proton-rich nuclei ^{26}P. The excitation energies and branching ratios of the low-lying proton-bound states were determined. A total of thirteen β-delayed γ-ray branches of ^{26}P were identified by five clover-type HPGe detectors. Compared with the information of its mirror nucleus, ^{26}P was investigated for the mirror asymmetries. The mirror asymmetry parameter for the first 2^+ excited state of ^{26}Si and ^{26}Mg extracted from this experiment was deduced to be 46(13)%, which is well reproduced by the shell-model calculations considering the weakly bound effect in both the Hamiltonian and the wave function. Our results and the observation by Pérez-Loureiro [14] support the conclusion that the large mirror asymmetry is close to the proton halo structure in ^{26}P.

We wish to acknowledge the support of the HIRFL operations staff for providing high-quality beams and the effort of the RIBLL1 collaborators in performing the experiment.

Author Contributions: Data curation, X.X., P.L. (Pengfei Liang), G.S., L.S., C.L., J.L. (Jenny Lee), Z.L., Y.Y. (Yanyun Yang), P.L. (Pengjie Li), R.F., S.Z., H.Z. (Haofan Zhu), J.L. (Jinhai Li), Z.Z., Q.G., R.C., J.W. (Jiansong Wang), D.W., H.W., K.W., F.D. (Fangfang Duan), Y.L. (Yihua Lam), P.M., Z.G., Q.H., Z.B., J.M., J.W. (Jianguo Wang), F.Z., C.W., D.L., Y.J., Y.L. (Yang Liu), D.H., R.L., N.M., W.M., G.Y., D.P. (Dipika Patel), S.J., Y.W., Y.Y. (Yuechao Yu), Q.Z. (Qingwu Zhou), P.W. (Peng Wang), L.H., X.W. (Xiang Wang), H.Z. (Hongliang Zang), Q.Z. (Qingqing Zhao), L.Y., P.W. (Peiwei Wen), F.Y., H.J. (Huiming Jia), G.Z., M.P., X.W. (Xiaoyu Wang), H.S. and W.Y.; Formal analysis, H.J. (Hao Jian) and Y.G.; Funding acquisition, X.X. and C.Y.; Methodology, C.Y., L.X. (Latsamy Xayavong), K.K. (Kazunari Kaneko) and Y.S.; Supervision, X.X., M.W., Z.H., X.Z., Y.Z., H.X., M.L. and H.-J.O.; Writing-original draft, Hao Jian and Y.G; Writing-review & editing, F.D. (Fanchao Dai), J.L. (Jiajian Liu), X.X. and C.Y. All authors have read and agreed to the published version of the manuscript.

Funding: This research was supported by the Strategic Priority Research Program of the Chinese Academy of Science grant number XDB34010300, the Ministry of Science and Technology of China under National Key R&D Programs grant numbers 2018YFA0404404 and 2016YFA0400503, National Natural Science Foundation of China grant numbers 11775316, 12022501, U1932206 and U1632136, and the Heavy Ion Research Facility in Lanzhou (HIRFL) grant number HIR2021ZD001.

Institutional Review Board Statement: Not applicable.

Informed Consent Statement: Not applicable.

Data Availability Statement: The data presented in this study are available in the article.

Conflicts of Interest: The authors declare no conflict of interest.

Abbreviations

The following abbreviations are used in this manuscript:

HIRFL	Heavy Ion Research Facility in Lanzhou
RIBLL1	Radioactive Ion Beam Line in Lanzhou
INC	isospin nonconserving
DSSD	double-sided silicon strip detector
QSD	quadrant silicon detector
HPGe	high-purity germanium
CSA	charge sensitive amplifier
PCB	printed circuit board
DAQ	data acquisition system
MED	mirror energy difference

References

1. Heisenberg, W. On the structure of atomic nuclei. *Z. Fur Phys.* **1932**, *77*, 1–11. [CrossRef]
2. Warner, D.D; Bentley, M.A.; Isacker, P.V. The role of isospin symmetry in collective nuclear structure. *Nat. Phys.* **2006**, *2*, 311–318. [CrossRef]
3. Bentley, M.; Lenzi, S.M. Coulomb energy differences between high-spin states in isobaric multiplets. *Prog. Part. Nucl. Phys.* **2007**, *59*, 497–561. [CrossRef]
4. Hoff, D.E.M.; Rogers, A.M.; Wang, S.M.; Bender, P.C.; Brandenburg, K.; Clark, J.A.; Dombos, A.C.; Doucet, E.R.; Jin, S.; et al. Mirror-symmetry violation in bound nuclear ground states. *Nature* **2020**, *580*, 52–55. [CrossRef]
5. Kaneko, K.; Sun, Y.; Mizusaki, T.; Jenkins, D.G.; Ghorui, S.K.; Tazaki, S. Large mirror asymmetry in Gamow–Teller β-decay in the A = 26 isobaric multiplets. *Nucl. Phys. A* **2019**, *986*, 107–115. [CrossRef]
6. Tanihata, I.; Savajols, H.; Kanungo, R. Recent experimental progress in nuclear halo structure studies. *Prog. Part. Nucl. Phys.* **2013**, *68*, 215–313. [CrossRef]
7. Wu, C.G.; Wu, H.Y.; Li, J.G.; Luo, D.W.; Li, Z.H.; Xu, X.X.; Lin, C.J.; Lee, J.; Sun, L.J.; Liang, P.F.; et al. β-decay spectroscopy of the proton drip-line nucleus ^{22}Al. *Phys. Rev. C* **2021**, *104*, 044311. [CrossRef]
8. Lee, J.; Xu, X.X.; Kaneko, K.; Sun, Y.; Lin, C.J.; Sun, L.J.; Liang, P.F.; Li, Z.H.; Li, J.; Wu, H.Y.; et al. Large Isospin Asymmetry in ^{22}Si/^{22}O Mirror Gamow–Teller Transitions Reveals the Halo Structure of ^{22}Al. *Phys. Rev. Lett.* **2020**, *125*, 192503. [CrossRef]
9. Sun, L.J.; Xu, X.X.; Lin, C.J.; Lee, J.; Hou, S.Q.; Yuan, C.X.; Li, Z.H.; José, J.; He, J.J.; Wang, J.S.; et al. β-decay spectroscopy of ^{27}S. *Phys. Rev. C* **2019**, *99*, 064312. [CrossRef]
10. Wang, Y.T.; Fang, D.Q.; Wang, K.; Xu, X.X.; Sun, L.J.; Bai, Z.; Bao, P.F.; Cao, X.G.; Dai, Z.T.; Ding, B.; et al. β-delayed particle emission from ^{21}Mg. *Eur. Phys. J. A* **2018**, *54*, 107. [CrossRef]
11. Wang, Y.T.; Fang, D.Q.; Xu, X.X.; Sun, L.J.; Wang, K.; Bao, P.F.; Bai, Z.; Cao, X.G.; Dai, Z.T.; Ding, B.; et al. Implantation-decay method to study the β-delayed charged particle decay. *Nucl. Sci. Tech.* **2018**, *29*, 98. [CrossRef]
12. Sun, L.J.; Xu, X.X.; Fang, D.Q.; Lin, C.J.; Wang, J.S.; Li, Z.H.; Wang, Y.T.; Li, J.; Yang, L.; Ma, N.R.; et al. β-decay study of the $T_Z = -2$ proton-rich nucleus ^{20}Mg. *Phys. Rev. C* **2017**, *95*, 014314. [CrossRef]
13. Xu, X.X.; Lin, C.J.; Sun, L.J.; Wang, J.S.; Lam, Y.H.; Lee, J.; Fang, D.Q.; Li, Z.H.; Smirnova, N.A.; Yuan, C.X.; et al. Observation of β-delayed two-proton emission in the decay of ^{22}Si. *Phys. Lett. B* **2017**, *766*, 312–316. [CrossRef]
14. Pérez-Loureiro, D.; Wrede, C.; Bennett, M.B.; Liddick, S.N.; Bowe, A.; Brown, B.A.; Chen, A.A.; Chipps, K.A.; Cooper, N.; Irvine, D.; et al. β-delayed γ decay of ^{26}P: Possible evidence of a proton halo. *Phys. Rev. C* **2016**, *93*, 064320. [CrossRef]
15. Ichikawa, Y.; Onishi, T.K.; Suzuki, D.; Iwasaki, H.; Kubo, T.; Naik, V.; Chakrabarti, A.; Aoi, N.; Brown, B.A.; Fukuda, N.; et al. Proton-rich nuclear structure and mirror asymmetry investigated by β-decay spectroscopy of ^{24}Si. *J. Phys. Conf. Ser.* **2011**, *312*, 092031. [CrossRef]
16. Zhan, W.L.; Xia, J.W.; Zhao, H.W.; Xiao, G.Q.; Yuan, Y.J.; Xu, H.S.; Man, K.D.; Yuan, P.; Gao, D.Q.; Yang, X.T.; et al. HIRFL Today. *Nucl. Phys. A* **2008**, *805*, 533c–540c. [CrossRef]
17. Sun, Z.; Zhan, W.L.; Guo, Z.Y.; Xiao, G.; Li, J.X. RIBLL, the radioactive ion beam line in Lznzhou. *Nucl. Instruments Methods Phys. Res. Sect. A* **2003**, *503*, 496–503. [CrossRef]
18. Tarasov, O.B.; Bazin, D. LISE++: Radioactive beam production with in-flight separators. *Nucl. Instruments Methods Phys. Res. Sect. B* **2008**, *266*, 4657–4664. [CrossRef]
19. Liang, P.F.; Sun, L.J.; Lee, J.; Hou, S.Q.; Xu, X.X.; Lin, C.J.; Yuan, C.X.; He, J.J.; Li, Z.H.; Wang, J.S.; et al. Simultaneous measurement of β-delayed proton and γ emission of ^{26}P for the ^{25}Al(p,γ) ^{26}Si reaction rate. *Phys. Rev. C* **2020**, *101*, 024305. [CrossRef]
20. Xu, X,X.; Teh, F.C.E.; Lin, C.J.; Lee, J.; Yang, F.; Guo, Z.Q.; Guo, T.S.; Sun, L.J.; Teng, X.Z.; Liu, J.J.; et al. Characterization of CIAE developed double-sided silicon strip detector for charged particles. *Nucl. Sci. Tech.* **2018**, *29*, 73. [CrossRef]
21. Bao, P.F.; Lin, C.J.; Yang, F.; Guo, Z.Q.; Guo, T.S.; Yang, L.; Sun, L.J.; Jia, H.M.; Xu, X.X.; Ma, N.R. Development of large-area quadrant silicon detector for charged particles. *Chin. Phys. C* **2014**, *38*, 126001. [CrossRef]
22. Sun, L.J.; Xu, X.X.; Lin, C.J.; Wang, J.S.; Fang, D.Q.; Li, Z.H.; Wang, Y.T.; Li, J.; Yang, L.; Ma, N.R.; et al. A detection system for chaeged-particle decay studies with a continuous-implantation method. *Nucl. Instruments Methods Phys. Res. Sect. A Accerators Spectrometers Detect. Assoc. Equip.* **2015**, *804*, 1–7. [CrossRef]
23. Baba, H.; Ichihara, T.; Ohnishi, T.; Takeuchi, S.; Yoshida, K.; Watanabe, Y.; Ota, S.; Shimoura, S. New data acquisition system for the RIKEN radioactive Isotope Beam Factory. *Nucl. Instruments Methods Phys. Res. Sect. A Accerators Spectrometers Detect. Assoc. Equip.* **2010**, *616*, 65–68. [CrossRef]
24. Thomas, J.C.; Achouri, L.; Aysto, J.; Beraud, R.; Blank, B.; Canchel, G.; Czajkowski, S.; Dendooven, P.; Ensallem, A.; Giovinazzo, J.; et al. Beta-decay properties ^{25}Si and ^{26}P. *Eur. Phys. J. A* **2004**, *21*, 419–435. [CrossRef]
25. Ziegler, J.F.; Ziegler, M.D.; Biersack, J.P. SRIM-The stopping and range of ions in matter. *Nucl. Instruments Methods Phys. Res. Sect. B Beam Interact. Mater. Atoms.* **2010**, *268*, 1818–1823. [CrossRef]
26. Bergmann, U.C.; Riisager, K. New statistical methods for exotic nuclei. *Nucl. Phys. A* **2002**, *701*, 213–216. [CrossRef]
27. Achouri, N.L.; de Oliveira Santos, F.; Lewitowicz, M.; Blank, B.; Aysto, J.; Canchel, G.; Czajkowski, S.; Dendooven, P.; Emsallem, A.; Giovinazzo, J.; et al. The β-decay of ^{22}Al. *Eur. Phys. J. A* **2006**, *27*, 287–300. [CrossRef]
28. Gove, N.B.; Martin, M.J. Log-ftables for beta decay. *At. Data Nucl. Data Tables* **1971**, *10*, 205–219. [CrossRef]
29. Zuker, A.P.; Lenzi, S.M.; Martínez-Pinedo, G.; Poves, A. Isobaric Multiplet Yrast Energies and Isospin Nonconserving Forces. *Phys. Rev. Lett.* **2002**, *89*, 142502. [CrossRef]

30. Kaneko, K.; Sun, Y.; Mizusaki, T.; Tazaki, S. Isospin nonconserving interaction in the $T = 1$ analogue states of the mass-70 region. *Phys. Rev. C* **2014**, *89*, 031302. [CrossRef]
31. Basunia, M.S.; Hurst, A.M. Nuclear Data Sheets for A = 26. *Nucl. Data Sheets* **2016**, *134*, 1–148. [CrossRef]
32. Hardy, J.C.; Towner, I.S. Superallowed $0^+ \to 0^+$ nuclear β decays: A new survey with precision tests of the conserved vector current hypothesis and the standard model. *Phys. Rev. C* **2009**, *79*, 055502. [CrossRef]
33. Wildenthal, B.H. Empirical strengths of spin operators in nuclei. *Prog. Part. Nucl. Phys.* **1984**, *11*, 5–51. [CrossRef]
34. Brown, B.A.; Wildenthal, B.H. Status of the nuclear shell model. *Annu. Rev. Nucl. Part. Sci.* **1988**, *38*, 29–66. [CrossRef]
35. Brown, B.A.; Richter, W.A. New "USD" Hamiltonians for the *sd* shell. *Phys. Rev. C* **2006**, *74*, 034315. [CrossRef]
36. Yuan, C.X.; Qi, C.; Xu, F.R.; Suzuki, T.; Otsuka, T. Mirror energy difference and the structure of loosely bound proton-rich nuclei around A = 20. *Phys. Rev. C* **2014**, *89*, 044327. [CrossRef]
37. Thomas, R.G. An Analysis of the Energy Levels of the mirror Nuclei, C^{13} and N^{13}. *Phys. Rev.* **1952**, *88*, 1109. [CrossRef]
38. Ehrman, J.B. On the Displacement of Corresponding Energy Levels of C^{13} and N^{13}. *Phys. Rev.* **1951**, *81*, 412. [CrossRef]